

Search for the lepton-flavor-violating decay $B^0 \rightarrow K^{*0} \mu^\pm e^\mp$

S. Sandilya,⁸ K. Trabelsi,^{19,15} A. J. Schwartz,⁸ I. Adachi,^{19,15} H. Aihara,⁸⁹ S. Al Said,^{83,39} D. M. Asner,⁴ H. Atmacan,⁷⁹ V. Aulchenko,^{5,68} T. Aushev,⁵⁷ R. Ayad,⁸³ V. Babu,⁸⁴ I. Badhrees,^{83,38} S. Bahinipati,²⁴ A. M. Bakich,⁸² V. Bansal,⁷⁰ P. Behera,²⁷ C. Beleño,¹⁴ V. Bhardwaj,²³ B. Bhuyan,²⁵ T. Bilka,⁶ J. Biswal,³⁵ A. Bobrov,^{5,68} A. Bozek,⁶⁵ M. Bračko,^{51,35} T. E. Browder,¹⁸ L. Cao,³⁶ D. Červenkov,⁶ P. Chang,⁶⁴ V. Chekelian,⁵² A. Chen,⁶² B. G. Cheon,¹⁷ K. Chilikin,⁴⁶ K. Cho,⁴⁰ S.-K. Choi,¹⁶ Y. Choi,⁸¹ S. Choudhury,²⁶ D. Cinabro,⁹³ S. Cunliffe,⁹ N. Dash,²⁴ S. Di Carlo,⁴⁴ J. Dingfelder,³ Z. Doležal,⁶ T. V. Dong,^{19,15} Z. Drásal,⁶ S. Eidelman,^{5,68,46} D. Epifanov,^{5,68} J. E. Fast,⁷⁰ T. Ferber,⁹ B. G. Fulsom,⁷⁰ R. Garg,⁷¹ V. Gaur,⁹² N. Gabyshev,^{5,68} A. Garmash,^{5,68} M. Gelb,³⁶ A. Giri,²⁶ P. Goldenzweig,³⁶ B. Golob,^{47,35} D. Greenwald,⁸⁵ Y. Guan,^{28,19} J. Haba,^{19,15} T. Hara,^{19,15} K. Hayasaka,⁶⁷ H. Hayashii,⁶¹ S. Hirose,⁵⁸ W.-S. Hou,⁶⁴ C.-L. Hsu,⁸² T. Iijima,^{59,58} K. Inami,⁵⁸ G. Inguglia,⁹ A. Ishikawa,⁸⁷ R. Itoh,^{19,15} M. Iwasaki,⁶⁹ Y. Iwasaki,¹⁹ W. W. Jacobs,²⁸ I. Jaegle,¹⁰ H. B. Jeon,⁴³ S. Jia,² Y. Jin,⁸⁹ D. Joffe,³⁷ K. K. Joo,⁷ T. Julius,⁵³ A. B. Kaliyar,²⁷ K. H. Kang,⁴³ T. Kawasaki,⁶⁷ H. Kichimi,¹⁹ C. Kiesling,⁵² D. Y. Kim,⁷⁸ J. B. Kim,⁴¹ K. T. Kim,⁴¹ S. H. Kim,¹⁷ K. Kinoshita,⁸ P. Kodyš,⁶ S. Korpar,^{51,35} D. Kotchetkov,¹⁸ P. Križan,^{47,35} R. Kroeger,⁵⁴ P. Krokovny,^{5,68} T. Kuhr,⁴⁸ R. Kulasiri,³⁷ R. Kumar,⁷⁴ A. Kuzmin,^{5,68} Y.-J. Kwon,⁹⁵ J. S. Lange,¹² I. S. Lee,¹⁷ S. C. Lee,⁴³ L. K. Li,²⁹ Y. B. Li,⁷² L. Li Gioi,⁵² J. Libby,²⁷ D. Liventsev,^{92,19} M. Lubej,³⁵ M. Masuda,⁸⁸ T. Matsuda,⁵⁵ D. Matvienko,^{5,68,46} M. Merola,^{32,60} K. Miyabayashi,⁶¹ H. Miyata,⁶⁷ R. Mizuk,^{46,56,57} G. B. Mohanty,⁸⁴ H. K. Moon,⁴¹ T. Mori,⁵⁸ R. Mussa,³³ E. Nakano,⁶⁹ M. Nakao,^{19,15} T. Nanut,³⁵ K. J. Nath,²⁵ Z. Natkaniec,⁶⁵ M. Nayak,^{93,19} M. Niiyama,⁴² N. K. Nisar,⁷³ S. Nishida,^{19,15} K. Ogawa,⁶⁷ S. Ogawa,⁸⁶ H. Ono,^{66,67} P. Pakhlov,^{46,56} G. Pakhlova,^{46,57} B. Pal,⁴ S. Pardi,³² S. Paul,⁸⁵ T. K. Pedlar,⁴⁹ R. Pestotnik,³⁵ L. E. Piilonen,⁹² V. Popov,^{46,57} K. Prasanth,⁸⁴ E. Prencipe,²¹ M. V. Purohit,⁷⁹ A. Rabusov,⁸⁵ P. K. Resmi,²⁷ A. Rostomyan,⁹ G. Russo,³² D. Sahoo,⁸⁴ Y. Sakai,^{19,15} M. Salehi,^{50,48} L. Santelj,¹⁹ T. Sanuki,⁸⁷ V. Savinov,⁷³ O. Schneider,⁴⁵ G. Schnell,^{1,22} C. Schwanda,³⁰ Y. Seino,⁶⁷ K. Senyo,⁹⁴ O. Seon,⁵⁸ M. E. Sevior,⁵³ C. P. Shen,² T.-A. Shibata,⁹⁰ J.-G. Shiu,⁶⁴ B. Shwartz,^{5,68} J. B. Singh,⁷¹ A. Sokolov,³¹ E. Solovieva,^{46,57} M. Starič,³⁵ J. F. Strube,⁷⁰ M. Sumihama,¹³ K. Sumisawa,^{19,15} T. Sumiyoshi,⁹¹ W. Sutcliffe,³⁶ M. Takizawa,^{77,20,75} U. Tamponi,³³ K. Tanida,³⁴ F. Tenchini,⁵³ M. Uchida,⁹⁰ T. Uglov,^{46,57} Y. Unno,¹⁷ S. Uno,^{19,15} P. Urquijo,⁵³ Y. Ushiroda,^{19,15} Y. Usov,^{5,68} C. Van Hulse,¹ R. Van Tonder,³⁶ G. Varner,¹⁸ A. Vinokurova,^{5,68} V. Vorobyev,^{5,68,46} E. Waheed,⁵³ B. Wang,⁸ C. H. Wang,⁶³ M.-Z. Wang,⁶⁴ P. Wang,²⁹ X. L. Wang,¹¹ S. Watanuki,⁸⁷ S. Wehle,⁹ E. Widmann,⁸⁰ E. Won,⁴¹ H. Yamamoto,⁸⁷ H. Ye,⁹ J. H. Yin,²⁹ C. Z. Yuan,²⁹ Y. Yusa,⁶⁷ Z. P. Zhang,⁷⁶ V. Zhilich,^{5,68} V. Zhukova,^{46,56} V. Zhulanov,^{5,68} and A. Zupanc^{47,35}

(Belle Collaboration)

¹University of the Basque Country UPV/EHU, 48080 Bilbao²Beihang University, 100191 Beijing³University of Bonn, 53115 Bonn⁴Brookhaven National Laboratory, Upton, 11973 New York⁵Budker Institute of Nuclear Physics SB RAS, 630090 Novosibirsk⁶Faculty of Mathematics and Physics, Charles University, 121 16 Prague⁷Chonnam National University, 660-701 Kwangju⁸University of Cincinnati, Cincinnati, 45221 Ohio⁹Deutsches Elektronen-Synchrotron, 22607 Hamburg¹⁰University of Florida, Gainesville, 32611 Florida¹¹Key Laboratory of Nuclear Physics and Ion-beam Application (MOE) and Institute of Modern Physics, Fudan University, 200443 Shanghai¹²Justus-Liebig-Universität Gießen, 35392 Gießen¹³Gifu University, 501-1193 Gifu¹⁴II. Physikalisches Institut, Georg-August-Universität Göttingen, 37073 Göttingen¹⁵SOKENDAI (The Graduate University for Advanced Studies), 240-0193 Hayama¹⁶Gyeongsang National University, 660-701 Chinju¹⁷Hanyang University, 133-791 Seoul¹⁸University of Hawaii, Honolulu, 96822 Hawaii¹⁹High Energy Accelerator Research Organization (KEK), 305-0801 Tsukuba²⁰J-PARC Branch, KEK Theory Center, High Energy Accelerator Research Organization (KEK), 305-0801 Tsukuba²¹Forschungszentrum Jülich, 52425 Jülich²²IKERBASQUE, Basque Foundation for Science, 48013 Bilbao²³Indian Institute of Science Education and Research Mohali, 140306 SAS Nagar

- ²⁴Indian Institute of Technology Bhubaneswar, 751007 Satya Nagar
²⁵Indian Institute of Technology Guwahati, 781039 Assam
²⁶Indian Institute of Technology Hyderabad, 502285 Telangana
²⁷Indian Institute of Technology Madras, 600036 Chennai
²⁸Indiana University, Bloomington, 47408 Indiana
²⁹Institute of High Energy Physics, Chinese Academy of Sciences, 100049 Beijing
³⁰Institute of High Energy Physics, 1050 Vienna
³¹Institute for High Energy Physics, 142281 Protvino
³²INFN - Sezione di Napoli, 80126 Napoli
³³INFN - Sezione di Torino, 10125 Torino
³⁴Advanced Science Research Center, Japan Atomic Energy Agency, 319-1195 Naka
³⁵J. Stefan Institute, 1000 Ljubljana
³⁶Institut für Experimentelle Teilchenphysik, Karlsruhe Institut für Technologie, 76131 Karlsruhe
³⁷Kennesaw State University, Kennesaw, 30144 Georgia
³⁸King Abdulaziz City for Science and Technology, 11442 Riyadh
³⁹Department of Physics, Faculty of Science, King Abdulaziz University, 21589 Jeddah
⁴⁰Korea Institute of Science and Technology Information, 305-806 Daejeon
⁴¹Korea University, 136-713 Seoul
⁴²Kyoto University, 606-8502 Kyoto
⁴³Kyungpook National University, 702-701 Daegu
⁴⁴LAL, Univ. Paris-Sud, CNRS/IN2P3, Université Paris-Saclay, Orsay
⁴⁵École Polytechnique Fédérale de Lausanne (EPFL), 1015 Lausanne
⁴⁶P.N. Lebedev Physical Institute of the Russian Academy of Sciences, 119991 Moscow
⁴⁷Faculty of Mathematics and Physics, University of Ljubljana, 1000 Ljubljana
⁴⁸Ludwig Maximilians University, 80539 Munich
⁴⁹Luther College, Decorah, 52101 Iowa
⁵⁰University of Malaya, 50603 Kuala Lumpur
⁵¹University of Maribor, 2000 Maribor
⁵²Max-Planck-Institut für Physik, 80805 München
⁵³School of Physics, University of Melbourne, 3010 Victoria
⁵⁴University of Mississippi, University, 38677 Mississippi
⁵⁵University of Miyazaki, 889-2192 Miyazaki
⁵⁶Moscow Physical Engineering Institute, 115409 Moscow
⁵⁷Moscow Institute of Physics and Technology, 141700 Moscow Region
⁵⁸Graduate School of Science, Nagoya University, 464-8602 Nagoya
⁵⁹Kobayashi-Maskawa Institute, Nagoya University, 464-8602 Nagoya
⁶⁰Università di Napoli Federico II, 80055 Napoli
⁶¹Nara Women's University, 630-8506 Nara
⁶²National Central University, 32054 Chung-li
⁶³National United University, 36003 Miao Li
⁶⁴Department of Physics, National Taiwan University, 10617 Taipei
⁶⁵H. Niewodniczanski Institute of Nuclear Physics, 31-342 Krakow
⁶⁶Nippon Dental University, 951-8580 Niigata
⁶⁷Niigata University, 950-2181 Niigata
⁶⁸Novosibirsk State University, 630090 Novosibirsk
⁶⁹Osaka City University, 558-8585 Osaka
⁷⁰Pacific Northwest National Laboratory, Richland, 99352 Washington
⁷¹Panjab University, 160014 Chandigarh
⁷²Peking University, 100871 Beijing
⁷³University of Pittsburgh, Pittsburgh, 15260 Pennsylvania
⁷⁴Punjab Agricultural University, 141004 Ludhiana
⁷⁵Theoretical Research Division, Nishina Center, RIKEN, 351-0198 Saitama
⁷⁶University of Science and Technology of China, 230026 Hefei
⁷⁷Showa Pharmaceutical University, 194-8543 Tokyo
⁷⁸Soongsil University, 156-743 Seoul
⁷⁹University of South Carolina, Columbia, 29208 South Carolina
⁸⁰Stefan Meyer Institute for Subatomic Physics, 1090 Vienna
⁸¹Sungkyunkwan University, 440-746 Suwon
⁸²School of Physics, University of Sydney, 2006 New South Wales
⁸³Department of Physics, Faculty of Science, University of Tabuk, 71451 Tabuk

⁸⁴*Tata Institute of Fundamental Research, 400005 Mumbai*⁸⁵*Department of Physics, Technische Universität München, 85748 Garching*⁸⁶*Toho University, 274-8510 Funabashi*⁸⁷*Department of Physics, Tohoku University, 980-8578 Sendai*⁸⁸*Earthquake Research Institute, University of Tokyo, 113-0032 Tokyo*⁸⁹*Department of Physics, University of Tokyo, 113-0033 Tokyo*⁹⁰*Tokyo Institute of Technology, 152-8550 Tokyo*⁹¹*Tokyo Metropolitan University, 192-0397 Tokyo*⁹²*Virginia Polytechnic Institute and State University, Blacksburg, 24061 Virginia*⁹³*Wayne State University, Detroit, 48202 Michigan*⁹⁴*Yamagata University, 990-8560 Yamagata*⁹⁵*Yonsei University, 120-749 Seoul*

(Received 10 July 2018; published 9 October 2018)

We have searched for the lepton-flavor-violating decay $B^0 \rightarrow K^{*0} \mu^\pm e^\mp$ using a data sample of 711 fb^{-1} that contains $772 \times 10^6 B\bar{B}$ pairs. The data were collected near the $\Upsilon(4S)$ resonance with the Belle detector at the KEKB asymmetric-energy e^+e^- collider. No signals were observed, and we set 90% confidence level upper limits on the branching fractions of $\mathcal{B}(B^0 \rightarrow K^{*0} \mu^+ e^-) < 1.2 \times 10^{-7}$, $\mathcal{B}(B^0 \rightarrow K^{*0} \mu^- e^+) < 1.6 \times 10^{-7}$, and, for both decays combined, $\mathcal{B}(B^0 \rightarrow K^{*0} \mu^\pm e^\mp) < 1.8 \times 10^{-7}$. These are the most stringent limits on these decays to date.

DOI: [10.1103/PhysRevD.98.071101](https://doi.org/10.1103/PhysRevD.98.071101)

In recent years, measurements from the LHCb [1,2] experiment have exhibited possible deviations from lepton universality in flavor-changing neutral-current $b \rightarrow s \ell^+ \ell^-$ transitions. Such universality is an important symmetry of the Standard Model. These deviations have generated much interest within the theoretical community, and several models of new physics [3–10] have been proposed to explain these discrepancies. In many such models, violation of lepton universality is accompanied by lepton flavor violation (LFV) [11]. The idea of LFV in B decays was discussed in Refs. [12–19]. Experimentally, one way to search for LFV is via the decays $B^0 \rightarrow K^{*0} \mu^\pm e^\mp$ [20], which have large available phase space and also avoid the helicity suppression that a two-body decay such as $B^0 \rightarrow \mu^\pm e^\mp$ might be subjected to. The most stringent upper limits for $B^0 \rightarrow K^{*0} \mu^\pm e^\mp$ were set by the BABAR experiment based on a data sample of $229 \times 10^6 B\bar{B}$ events [21]. Here, we report a search for $B^0 \rightarrow K^{*0} \mu^\pm e^\mp$ using a data sample of $(772 \pm 11) \times 10^6 B\bar{B}$ events (711 fb^{-1}), which is more than 3 times larger than that of BABAR. The data sample was collected by the Belle experiment running near the $\Upsilon(4S)$ resonance at the KEKB e^+e^- collider [22].

The Belle detector is a large-solid-angle magnetic spectrometer consisting of a silicon vertex detector (SVD), a 50-layer central drift chamber (CDC), an array of aerogel threshold Cherenkov counters (ACC), a barrel-like

arrangement of time-of-flight scintillation counters (TOF), and an electromagnetic calorimeter (ECL) comprising CsI (TI) crystals. All are located inside a superconducting solenoid coil, which provides a 1.5 T magnetic field. An iron flux return yoke located outside the coil is instrumented with resistive-plate chambers (KLM) to detect K_L^0 mesons and muons. Further details of the detector are given in Ref. [23]. Two inner detector configurations were used: a 2.0 cm radius beam-pipe and a three-layer SVD were used to record the first sample of 140 fb^{-1} , while a 1.5 cm radius beam-pipe, a four-layer SVD, and a small-cell inner drift chamber were used to record the remaining 571 fb^{-1} [24].

To study properties of signal events and optimize selection criteria, we generate samples of Monte Carlo (MC) simulated events. These samples are generated with the EVTGEN package [25] using three-body phase space and assuming that the K^{*0} is unpolarized. The detector response is simulated with the GEANT3 package [26].

We begin reconstructing $B^0 \rightarrow K^{*0} \mu^\pm e^\mp$ [27] decays by selecting charged particles that originate from a region near the e^+e^- interaction point. This region is defined using impact parameters: we require $dr < 1 \text{ cm}$ in the x - y plane (transverse to the positron beam), and $|dz| < 4 \text{ cm}$ along the z axis (antiparallel to the positron beam). To reduce backgrounds from low-momentum particles, we require that tracks have a transverse momentum (p_T) greater than $0.1 \text{ GeV}/c$.

From selected tracks, we identify K^\pm , π^\pm , μ^\pm , and e^\pm candidates using information from the CDC, ACC, and TOF detectors. The K^\pm and π^\pm candidates are identified by constructing the likelihood ratio $\mathcal{R}_K = \mathcal{L}_K / (\mathcal{L}_K + \mathcal{L}_\pi)$, where \mathcal{L}_π and \mathcal{L}_K are relative likelihoods for kaons and pions, respectively, calculated based on the number of

Published by the American Physical Society under the terms of the [Creative Commons Attribution 4.0 International license](https://creativecommons.org/licenses/by/4.0/). Further distribution of this work must maintain attribution to the author(s) and the published article's title, journal citation, and DOI. Funded by SCOAP³.

photoelectrons in the ACC, the specific ionization in the CDC, and the time-of-flight as determined from TOF hit times. We select kaons (pions) by requiring $\mathcal{R}_K > 0.6$ (< 0.4). This criterion is 92% (89%) efficient for kaons (pions), and has a misidentification rate of 7% (8%) for pions (kaons).

Muon candidates are identified based on information from the KLM detector. We require that candidates have momentum greater than 0.8 GeV/ c , and that they have a penetration depth and degree of transverse scattering consistent with those of a muon, given the track momentum measured in the CDC [28]. A criterion on normalized muon likelihood, $\mathcal{R}_\mu > 0.9$, is used to select muon candidates. For this requirement, the average muon detection efficiency is 89%, and the average pion misidentification rate is 1.4% [29].

Electron candidates are required to have momentum greater than 0.4 GeV/ c and are identified using the following information: the ratio of ECL energy to the CDC track momentum; the ECL shower shape; position matching between the CDC track and the ECL cluster; the energy loss in the CDC; and the response of the ACC [30]. A requirement on normalized electron likelihood $\mathcal{R}_e > 0.9$ is imposed. This requirement has an efficiency of 92% and a pion misidentification rate of about 0.25% [29]. To recover electron energy lost due to possible bremsstrahlung, we search for photons inside a cone of radius 50 mrad centered around the electron momentum. If a photon is found within this cone, its four-momentum is added to that of the electron.

Kaon and pion candidates are combined to form K^{*0} candidates by requiring that their K - π invariant mass be within a 100 MeV/ c^2 window centered around the K^{*0} mass [31]. B candidates are subsequently reconstructed by combining K^{*0} , μ^\pm , and e^\mp candidates. To discriminate signal decays from background, two kinematic variables are defined: the beam-energy-constrained mass $M_{bc} = \sqrt{(E_{\text{beam}}/c^2)^2 - (p_B/c)^2}$, and the energy difference $\Delta E = E_B - E_{\text{beam}}$, where E_{beam} is the beam energy and E_B and p_B are the energy and momentum, respectively, of the B candidate. All of these quantities are evaluated in the e^+e^- center-of-mass (CM) frame. For signal events, the ΔE distribution peaks near zero, and the M_{bc} distribution peaks near the B mass. We retain events satisfying the loose requirements $\Delta E \in [-0.05, 0.04]$ GeV and $M_{bc} > 5.2$ GeV/ c^2 .

After the above selection criteria are imposed, about 3% of events have more than one signal B candidate. To select a single candidate, we choose the one with the smallest χ^2 from a vertex fit of the four charged tracks. From MC simulation, we find that this criterion identifies the correct signal decay 63% of the time.

At this stage of the analysis, there is significant background from $e^+e^- \rightarrow q\bar{q}$ ($q = u, d, s, c$) continuum events. As lighter quarks are produced with large initial

momentum, these events tend to consist of two back-to-back jets of pions and kaons. In contrast, $e^+e^- \rightarrow b\bar{b}$ events result in $B\bar{B}$ pairs produced almost at rest in the CM frame; this results in more spherically distributed daughter particles. We thus distinguish $B\bar{B}$ events from $q\bar{q}$ background based on event topology. We use a multivariate analyzer constructed from a neural network (NN) that uses the following information:

- (1) A likelihood ratio constructed from modified Fox-Wolfram moments [32,33].
- (2) The angle between the thrust axis of the B decay products and that of the rest of the event (the thrust axis is defined as the direction that maximizes the sum of the longitudinal momenta of all particles).
- (3) The angle θ_B between the z axis and the B flight direction in the CM frame (for $B\bar{B}$ events, $dN/d\cos\theta_B \propto 1 - \cos^2\theta_B$, whereas for continuum events, $dN/d\cos\theta_B \approx \text{constant}$).
- (4) Flavor-tagging information from the other (non-signal) B decay. Our flavor-tagging algorithm [34] outputs two variables: the flavor q of the tag-side B , and the tag quality r . The latter ranges from zero for no flavor information to one for unambiguous flavor assignment.

We choose a selection criterion on the NN output ($\mathcal{O}_{\text{NN}}^{q\bar{q}}$) by optimizing a figure of merit $\varepsilon/\sqrt{N_B}$, where ε is the signal efficiency as determined from MC simulation, and N_B is the total number of background events expected in a restrictive signal region $M_{bc} > 5.27$ GeV/ c^2 . We obtain a criterion $\mathcal{O}_{\text{NN}}^{q\bar{q}} > 0.5$, which rejects 94% of $q\bar{q}$ background while retaining 73% of signal events.

After this criterion is applied, the remaining background arises mainly from B decays that produce two leptons. Such background falls into three categories: (a) both B and \bar{B} decay semileptonically; (b) a $B \rightarrow \bar{D}^{(*)}X\ell^+\nu$ decay is followed by a $\bar{D}^{(*)} \rightarrow X\ell^-\bar{\nu}$ decay; and (c) hadronic B decays where one or more daughter particles are misidentified as leptons. To suppress these backgrounds, we use a second NN that utilizes the following information:

- (1) The separation in z between the signal B decay vertex and the vertex of the other B .
- (2) The sum of the ECL energy of tracks and clusters *not* associated with the signal B decay.
- (3) The χ^2 of the vertex fit of the four charged tracks forming the signal- B decay vertex.
- (4) The separation in z between the two lepton tracks.

The criterion on the NN output, $\mathcal{O}_{\text{NN}}^{BB} > 0$, is obtained by maximizing the above figure of merit, $\varepsilon/\sqrt{N_B}$. At this stage, we also optimize the criterion on the variable ΔE , obtaining $|\Delta E| < 0.025$ GeV.

After applying this NN selection, only a small amount of background survives. We study this remaining background using MC simulation and find that the main source is $B^0 \rightarrow K^{*0}(\rightarrow K^+\pi^-)J/\psi(\rightarrow \ell^+\ell^-)$ decays in which one of

the leptons is misidentified and swapped with the K^+ or π^- . To suppress this background, we apply a set of vetoes. For $B^0 \rightarrow K^{*0}\mu^+e^-$ signal events, we apply three: the dilepton invariant mass must satisfy $M(\ell^+\ell^-) \notin [3.04, 3.12] \text{ GeV}/c^2$; the kaon-electron invariant mass must satisfy $M(K^+e^-) \notin [2.90, 3.12] \text{ GeV}/c^2$; and the pion-muon invariant mass must satisfy $M(\pi^-\mu^+) \notin [3.06, 3.12] \text{ GeV}/c^2$. For $B^0 \rightarrow K^{*0}\mu^-e^+$ signal events, we apply two vetoes: the dilepton invariant mass must satisfy $M(\ell^+\ell^-) \notin [3.02, 3.12] \text{ GeV}/c^2$, and the pion-electron invariant mass must satisfy $M(\pi^-e^+) \notin [3.02, 3.12] \text{ GeV}/c^2$. While calculating these invariant masses, the mass hypothesis for a hadron is taken to be that of the associated lepton. These vetoes have relative efficiencies of 90.4% and 94.8% for $B^0 \rightarrow K^{*0}\mu^+e^-$ and $B^0 \rightarrow K^{*0}\mu^-e^+$, respectively. We use a high-statistics MC sample to study backgrounds originating from charmless hadronic B decays and find them to be negligible. The largest contribution is from $B^0 \rightarrow K^{*0}\pi^+\pi^-$ in which the pions are misidentified as leptons; this contribution is only 0.01 event. To avoid bias, all selection criteria are determined in a “blind” manner, i.e., they are finalized before looking at events in the signal region.

To test our understanding of remaining backgrounds, we compare the M_{bc} distributions for data and MC events, as shown in Fig. 1. The plots show good agreement between data and MC for both the number of events observed and the shapes of the distributions.

We calculate the signal yield by performing an unbinned extended maximum-likelihood fit to the M_{bc} distribution. The probability density function (PDF) used to model signal decays is a Gaussian, and that for all backgrounds combined is an ARGUS function [35]. The signal shape parameters are obtained from MC simulation. We check these parameters by fitting the M_{bc} distribution of a control sample of $B^0 \rightarrow K^{*0}(\rightarrow K^+\pi^-)J/\psi(\rightarrow \ell^+\ell^-)$ decays. For this control sample, we fit both data and MC events and find excellent agreement between them for the shape parameters obtained. All background shape parameters, along with the signal and background yields, are floated in the fit. The fitted M_{bc} distributions are shown in Fig. 2. The fitted yields are $N_{\text{sig}} = -1.5^{+4.7}_{-4.1}$ and $0.4^{+4.8}_{-4.5}$ for $B^0 \rightarrow K^{*0}\mu^+e^-$ and $B^0 \rightarrow K^{*0}\mu^-e^+$, respectively. By combining both final states, we obtain $N_{\text{sig}} = -1.2^{+6.8}_{-6.2}$.

As there is no evidence of a signal, we calculate 90% confidence level (C.L.) upper limits on the branching fractions using a frequentist method as follows. We scan through a range of possible signal yields, and for each yield generate 10 000 sets of signal and background events according to their PDFs. Each set of events is statistically equivalent to our data set of 711 fb^{-1} . We combine signal

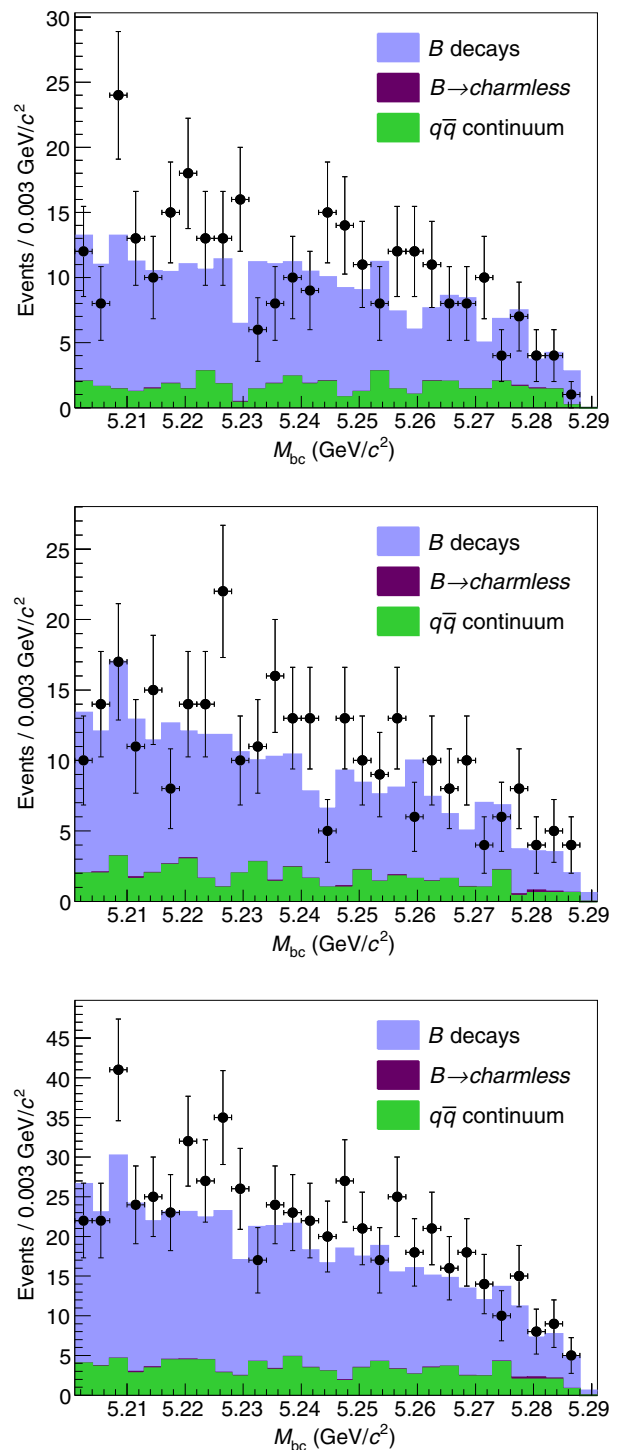


FIG. 1. The M_{bc} distribution for data and MC events that pass the selection criteria for the decays $B^0 \rightarrow K^{*0}\mu^+e^-$ (top), $B^0 \rightarrow K^{*0}\mu^-e^+$ (middle), and for both decays combined (bottom). Points with error bars are the data, while the color filled stacked histograms depict MC components from generic B decays (blue), $q\bar{q}$ continuum (green), and negligible contributions from charmless hadronic B decays (purple).

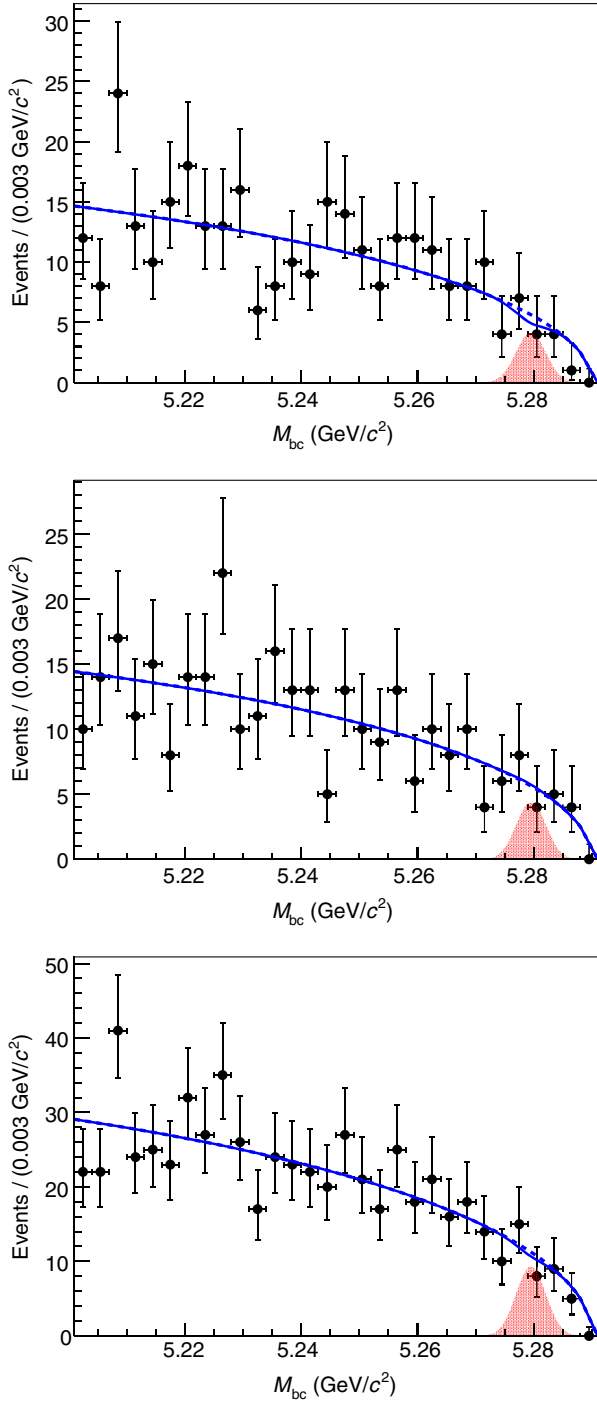


FIG. 2. The M_{bc} distribution for data events that pass the selection criteria for the decays $B^0 \rightarrow K^{*0}\mu^+e^-$ (top), $B^0 \rightarrow K^{*0}\mu^-e^+$ (middle), and also both decays combined (bottom). Points with error bars are the data, and the blue solid curve is the result of the fit for the signal-plus-background hypothesis, where the blue dashed curve is the background component. The red shaded histogram represents the signal PDF with arbitrary normalization.

and background samples and perform our fitting procedure on these combined sets of events. We then calculate, for each input value of signal yield, the fraction of sets (f_{sig})

TABLE I. Results from the fits. The rightmost columns correspond to efficiency, signal yield, 90% C.L. upper limit on the signal yield, and 90% C.L. upper limit on the branching fraction.

Mode	ϵ (%)	N_{sig}	$N_{\text{sig}}^{\text{UL}}$	\mathcal{B}^{UL} (10^{-7})
$B^0 \rightarrow K^{*0}\mu^+e^-$	8.8	$-1.5^{+4.7}_{-4.1}$	5.2	1.2
$B^0 \rightarrow K^{*0}\mu^-e^+$	9.3	$0.4^{+4.8}_{-4.5}$	7.4	1.6
$B^0 \rightarrow K^{*0}\mu^\pm e^\mp$ (combined)	9.0	$-1.2^{+6.8}_{-6.2}$	8.0	1.8

that have a fitted yield less than that observed in the data. The input signal having $f_{\text{sig}} = 0.10$ is taken as an upper limit $N_{\text{sig}}^{\text{UL}}$ (statistical error only). We convert $N_{\text{sig}}^{\text{UL}}$ into an upper limit on the branching fraction (\mathcal{B}^{UL}) via the formula

$$\mathcal{B} = \frac{N_{\text{sig}}}{\mathcal{B}(K^{*0} \rightarrow K^+\pi^-) \times 2 \times N_{B\bar{B}} \times f^{00} \times \epsilon},$$

where $\mathcal{B}(K^{*0} \rightarrow K^+\pi^-) = 0.6651$ is the assumed branching fraction (from isospin symmetry) for the intermediate decay $K^{*0} \rightarrow K^+\pi^-$; $N_{B\bar{B}}$ is the number of $B\bar{B}$ pairs, $(7.72 \pm 0.11) \times 10^8$; f^{00} is the branching fraction $\mathcal{B}(\Upsilon(4S) \rightarrow B^0\bar{B}^0) = 0.486 \pm 0.006$ [31]; and ϵ is the signal reconstruction efficiency as calculated from MC simulation. We include systematic uncertainty in \mathcal{B}^{UL} by smearing the N_{sig} distributions of the aforementioned statistically equivalent samples by the total fractional systematic uncertainty (see below) before calculating f_{sig} . The resulting upper limits are listed in Table I. For the upper limit on both decays $K^{*0}\mu^+e^-$ and $K^{*0}\mu^-e^+$ combined, $\mathcal{B}(B^0 \rightarrow K^{*0}\mu^\pm e^\mp) \equiv \mathcal{B}(B^0 \rightarrow K^{*0}\mu^+e^-) + \mathcal{B}(B^0 \rightarrow K^{*0}\mu^-e^+)$, and the branching fractions for the two modes are assumed to be identical when calculating the efficiency.

There are a number of systematic uncertainties, as listed in Table II. The uncertainty on ϵ due to limited MC

TABLE II. Systematic uncertainties included in calculating the upper limits.

Source	Systematic uncertainty (%)		
	$K^{*0}\mu^+e^-$	$K^{*0}\mu^-e^+$	$K^{*0}\mu^\pm e^\mp$
Reconstruction efficiency	± 0.3	± 0.3	± 0.3
Number of $B^0\bar{B}^0$ pairs	± 1.4	± 1.4	± 1.4
f^{00}	± 1.2	± 1.2	± 1.2
Track reconstruction	± 1.4	± 1.4	± 1.4
Particle identification	± 2.8	± 2.8	± 2.8
$\mathcal{O}_{\text{NN}}^{q\bar{q}}$ and $\mathcal{O}_{\text{NN}}^{\text{BB}}$	± 2.8	± 2.8	± 2.8
PDF shape parameters	+2.1 -3.0	+8.2 -8.1	+4.5 -4.5
$B \rightarrow$ charmless decays	± 0.5	± 2.2	± 1.4
K^{*0} polarization	+2.7 -1.4	+3.8 -1.9	+3.2 -1.6
Total	+5.7 -5.6	+10.3 -9.7	+7.2 -6.7

statistics is 0.3%, and the uncertainty on the number of $B^0\bar{B}^0$ pairs is 1.4%. The systematic uncertainties related to detector performance are determined from dedicated studies of control samples; specifically, these samples are used to measure tracking and particle identification efficiencies of charged particles. The systematic uncertainty due to charged track reconstruction is 0.35% per track. The uncertainty due to particle identification requirements is 2.8%. The uncertainty due to the requirements imposed on $\mathcal{O}_{\text{NN}}^{q\bar{q}}$ and $\mathcal{O}_{\text{NN}}^{\text{BB}}$ is evaluated by imposing the same requirements on the control sample of $B \rightarrow K^{*0}J/\psi, J/\psi \rightarrow \ell^+\ell^-$ decays. We compare the efficiencies of the \mathcal{O}_{NN} criteria on the control sample to those obtained from corresponding MC samples; the ratio is used to correct our signal efficiency, and the statistical error on the ratio is taken as the systematic uncertainty. For $\mathcal{O}_{\text{NN}}^{q\bar{q}}$, this ratio is 1.002 ± 0.022 ; for $\mathcal{O}_{\text{NN}}^{\text{BB}}$, the ratio is 0.919 ± 0.026 . The total systematic uncertainty due to both NN criteria applied together is 2.8%. The uncertainty due to the PDF shapes is evaluated by varying the fixed PDF shape parameters by $\pm 1\sigma$ and repeating the fit; the change in the central value of N_{sig} is taken as the systematic uncertainty. Systematic uncertainties due to the aforementioned tiny contribution of the charmless hadronic B decays are included. We initially assume that the K^{*0} is unpolarized. To investigate the effect of this, we calculate the reconstruction efficiency for fully longitudinal and fully transverse polarizations. The efficiency varies by only a few percent, and we include this variation as a systematic uncertainty.

Our reconstruction efficiency corresponds to $B^0 \rightarrow K^{*0}\mu^\pm e^\mp$ decays proceeding according to three-body phase space. The corresponding $q^2 \equiv M^2(\ell^+\ell^-)$ spectra peak at low values, where the reconstruction efficiency is also low; thus our upper limits are conservative. For larger values of q^2 , the efficiency rises approximately linearly from a minimum of 8% to 14% near q_{max}^2 . Such higher efficiencies would give lower upper limits.

In summary, we have searched for the lepton-flavor-violating decays $B^0 \rightarrow K^{*0}\mu^\pm e^\mp$ using the full Belle data set recorded at the $\Upsilon(4S)$ resonance. We see no statistically significant signal and set the following 90% C.L. upper limits on the branching fractions:

$$\mathcal{B}(B^0 \rightarrow K^{*0}\mu^+e^-) < 1.2 \times 10^{-7}, \quad (1)$$

$$\mathcal{B}(B^0 \rightarrow K^{*0}\mu^-e^+) < 1.6 \times 10^{-7}, \quad (2)$$

$$\mathcal{B}(B^0 \rightarrow K^{*0}\mu^\pm e^\mp) < 1.8 \times 10^{-7}. \quad (3)$$

These results are the most stringent constraints on these LFV decays to date.

ACKNOWLEDGMENTS

We thank the KEKB group for the excellent operation of the accelerator; the KEK cryogenics group for the efficient operation of the solenoid; and the KEK computer group, the National Institute of Informatics, and the Pacific Northwest National Laboratory (PNNL) Environmental Molecular Sciences Laboratory (EMSL) computing group for valuable computing and Science Information NETwork 5 (SINET5) network support. We acknowledge support from the Ministry of Education, Culture, Sports, Science, and Technology (MEXT) of Japan, the Japan Society for the Promotion of Science (JSPS), and the Tau-Lepton Physics Research Center of Nagoya University; the Australian Research Council; Austrian Science Fund under Grant No. P 26794-N20; the National Natural Science Foundation of China under Contracts No. 11435013, No. 11475187, No. 11521505, No. 11575017, No. 11675166, No. 11705209; Key Research Program of Frontier Sciences, Chinese Academy of Sciences (CAS), Grant No. QYZDJ-SSW-SLH011; the CAS Center for Excellence in Particle Physics (CCEPP); Fudan University Grant No. JIH5913023, No. IDH5913011/003, No. JIH5913024, No. IDH5913011/002; the Ministry of Education, Youth and Sports of the Czech Republic under Contract No. LTT17020; the Carl Zeiss Foundation, the Deutsche Forschungsgemeinschaft, the Excellence Cluster Universe, and the VolkswagenStiftung; the Department of Science and Technology of India; the Istituto Nazionale di Fisica Nucleare of Italy; National Research Foundation (NRF) of Korea Grants No. 2014R1A2A2A01005286, No. 2015R1A2A2A01003280, No. 2015H1A2A1033649, No. 2016R1D1A1B01010135, No. 2016K1A3A7A09005 603, No. 2016R1D1A1B02012900; Radiation Science Research Institute, Foreign Large-size Research Facility Application Supporting project and the Global Science Experimental Data Hub Center of the Korea Institute of Science and Technology Information; the Polish Ministry of Science and Higher Education and the National Science Center; the Ministry of Education and Science of the Russian Federation and the Russian Foundation for Basic Research; the Slovenian Research Agency; Ikerbasque, Basque Foundation for Science, Basque Government (No. IT956-16) and Ministry of Economy and Competitiveness (MINECO) (Juan de la Cierva), Spain; the Swiss National Science Foundation; the Ministry of Education and the Ministry of Science and Technology of Taiwan; and the United States Department of Energy and the National Science Foundation.

- [1] R. Aaij *et al.* (LHCb Collaboration), *Phys. Rev. Lett.* **113**, 151601 (2014).
- [2] R. Aaij *et al.* (LHCb Collaboration), *J. High Energy Phys.* **08** (2017) 055.
- [3] W. Altmannshofer, P. Ball, A. Bharucha, A. J. Buras, D. M. Straub, and M. Wick, *J. High Energy Phys.* **01** (2009) 019.
- [4] W. Altmannshofer and D. M. Straub, *Eur. Phys. J. C* **75**, 382 (2015).
- [5] S. Descotes-Genon, J. Matias, M. Ramon, and J. Virto, *J. High Energy Phys.* **01** (2013) 048.
- [6] S. Descotes-Genon, T. Hurth, J. Matias, and J. Virto, *J. High Energy Phys.* **05** (2013) 137.
- [7] S. Descotes-Genon, L. Hofer, J. Matias, and J. Virto, *J. High Energy Phys.* **12** (2014) 125.
- [8] B. Capdevila, S. Descotes-Genon, J. Matias, and J. Virto, *J. High Energy Phys.* **10** (2016) 075.
- [9] S. Descotes-Genon, L. Hofer, J. Matias, and J. Virto, *J. High Energy Phys.* **06** (2016) 092.
- [10] B. Capdevila, A. Crivellin, S. Descotes-Genon, J. Matias, and Javier Virto, *J. High Energy Phys.* **01** (2018) 093.
- [11] S. L. Glashow, D. Guadagnoli, and K. Lane, *Phys. Rev. Lett.* **114**, 091801 (2015).
- [12] D. Guadagnoli and K. Lane, *Phys. Lett. B* **751**, 54 (2015).
- [13] S. M. Boucenna, J. W. F. Valle, and A. Vicente, *Phys. Lett. B* **750**, 367 (2015).
- [14] B. Gripaios, M. Nardecchia, and S. A. Renner, *J. High Energy Phys.* **05** (2015) 006.
- [15] B. Bhattacharya, A. Datta, D. London, and S. Shivashankara, *Phys. Lett. B* **742**, 370 (2015).
- [16] S. Sahoo and R. Mohanta, *Phys. Rev. D* **91**, 094019 (2015).
- [17] I. de Medeiros Varzielas and G. Hiller, *J. High Energy Phys.* **06** (2015) 072.
- [18] D. Bečirević, O. Sumensari, and R. Z. Funchal, *Eur. Phys. J. C* **76**, 134 (2016).
- [19] A. Crivellin, D. Müller, A. Signer, and Y. Ulrich, *Phys. Rev. D* **97**, 015019 (2018).
- [20] The $K^*(892)^0$ is denoted as K^{*0} throughout this paper.
- [21] B. Aubert *et al.* (BABAR Collaboration), *Phys. Rev. D* **73**, 092001 (2006).
- [22] S. Kurokawa and E. Kikutani, *Nucl. Instrum. Methods Phys. Res., Sect. A* **499**, 1 (2003), and other papers included in this volume; T. Abe *et al.*, *Prog. Theor. Exp. Phys.* **2013**, 03A001 (2013) and following articles up to 03A011.
- [23] A. Abashian *et al.* (Belle Collaboration), *Nucl. Instrum. Methods Phys. Res., Sect. A* **479**, 117 (2002); also, see the detector section in J. Brodzicka *et al.*, *Prog. Theor. Exp. Phys.* **2012**, 04D001 (2012).
- [24] Z. Natkaniec *et al.* (Belle SVD2 Group Collaboration), *Nucl. Instrum. Methods Phys. Res., Sect. A* **560**, 1 (2006).
- [25] D. J. Lange, *Nucl. Instrum. Methods Phys. Res., Sect. A* **462**, 152 (2001).
- [26] R. Brun *et al.*, CERN Report No. DD/EE/84-1, 1984.
- [27] The inclusion of the charge conjugate decay mode is implied unless otherwise stated.
- [28] A. Abashian *et al.*, *Nucl. Instrum. Methods Phys. Res., Sect. A* **491**, 69 (2002).
- [29] E. Nakano, *Nucl. Instrum. Methods Phys. Res., Sect. A* **494**, 402 (2002).
- [30] K. Hanagaki, H. Kakuno, H. Ikeda, T. Iijima, and T. Tsukamoto, *Nucl. Instrum. Methods Phys. Res., Sect. A* **485**, 490 (2002).
- [31] C. Patrignani *et al.* (Particle Data Group Collaboration), *Chin. Phys. C* **40**, 100001 (2016) and 2017 update.
- [32] S. H. Lee *et al.* (Belle Collaboration), *Phys. Rev. Lett.* **91**, 261801 (2003).
- [33] G. C. Fox and S. Wolfram, *Phys. Rev. Lett.* **41**, 1581 (1978).
- [34] H. Kakuno *et al.* (Belle Collaboration), *Nucl. Instrum. Methods Phys. Res., Sect. A* **533**, 516 (2004).
- [35] H. Albrecht *et al.* (ARGUS Collaboration), *Phys. Lett. B* **241** (1990) 278.